CDF note 10936

A Direct Top Quark Width Measurement at CDF

The CDF Collaboration
URL http://www-cdf.fnal.gov
(Dated: November 9, 2012)

We present a measurement of top quark width using the full data set of CDF Run II corresponding to 8.7 fb^{-1} of Tevatron's $p\bar{p}$ collisions at Fermilab. We use a two dimensional template method to build the probability of signals and background in the lepton+jets decay topology. The observables are the reconstructed top quark mass from the minimization of a χ^2 for the overconstrained system, and the invariant mass of two jets from the hadronic W decays, which provides an *in situ* improvement in the determination of jet energy scale. We use a Feldman-Cousin (FC) construction method from Monte Carlo pseudo experiments and extract the top quark width from data. We measure the top quark width to be $\Gamma_{\rm top} = 2.21\ ^{+1.84}_{-1.11}$ GeV. This result corresponds to the top quark life time of $\tau_{\rm top} = 2.98^{+3.00}_{-1.35} \times 10^{-25}$ s. We also set an upper limit on the top quark width of $\Gamma_{\rm top} < 6.38$ GeV at 95% CL, which corresponds to a lower limit on the top quark life time of $\tau_{\rm top} > 1.03 \times 10^{-25}$ s at 95% CL.

Preliminary Results of the top quark width with 8.7 fb^{-1}

I. INTRODUCTION

This note describes a measurement of top quark width using $\bar{p}p$ collisions at $\sqrt{s} = 1.96$ TeV with the CDF detector at the Fermilab Tevatron. In Standard Model, a top quark decay is expected to be dominated by channel $t \to Wb$ according to CKM Quark-Mixing Matrix. The theoretical top decay width at next-to-leading order is[1]:

$$\Gamma_{\rm top} = \frac{G_F m_t^3}{8\pi\sqrt{2}} \left(1 - \frac{M_W^2}{m_t^2}\right)^2 \left(1 + 2\frac{M_W^2}{m_t^2}\right) \left[1 - \frac{2\alpha_s}{3\pi}\left(\frac{2\pi^2}{3} - \frac{5}{2}\right)\right] \quad (1)$$

which gives a short life time of 5×10^{-25} s and makes top quark decay before top-flavored hadrons or $t\bar{t}$-quarkonium-bound states can form[2]. According to Heisenberg Uncertainty Principle $\tau = \hbar/\Gamma$, the predicted top quark decay width is 1.25 GeV, which is out of the reach of the sensitivity of current experiments, and [3] gives a upper limit of top width $\Gamma_{\rm top} < 7.6$ GeV at 95% confidence level.

In this analysis, we use $t\bar{t}$ lepton+Jets channel and use a template method. We generate Monte Carlo (MC) samples using PYTHIA with dfferent input top widths ranging from 0.1 GeV to 30 GeV and all the samples have the same input top quark mass $\mathrm{M_{top}} = 172.5$ GeV/c^2. For each event in these samples an invariant top quark mass ($m_t^{\rm reco}$) and dijet mass of W boson (m_{jj}) are reconstructed, which form a two-dimentional template for each sample. The shape of $m_t^{\rm reco}$ will change as the input top width changes, as shown in Figure 1. By comparing the shapes (or distributions) of these two observables with that of the events drawn from samples (or data) with unknown top quark widths, we can extract the top quark width using maximum likelihood fit. We then perform Pseudo-Experiments (PE) for each MC sample, which enables us to apply Feldman-Cousins (FC) [4] construction to build confidence interval for the top quark width. In the Feldman-Cousins construction, we calculate the likelihood ratio,

$$R(x) = \frac{P(x|\Gamma_0)}{P(x|\Gamma_{max})}$$

, from the Monte-Carlo (ME) experiments, and obtain the confidence band with an ordering of the likelihood ratio for selecting the acceptance region. Where $R(x)$ is a likelihood ratio at x for a given width, Γ_0, and Γ_{max} is the width that yields the maximum likelihood among all the possible width. To incorporate systematic effects in to top quark width limits, we first convolute then shift the maximum likelihood function with and by a Gaussian function, which has a σ related to systematic effects. Thus a new maximum likelihood function with systematic effects considered is defined, and the same procedure as without systematic effects will be conducted afterwards to get top width limit(s).

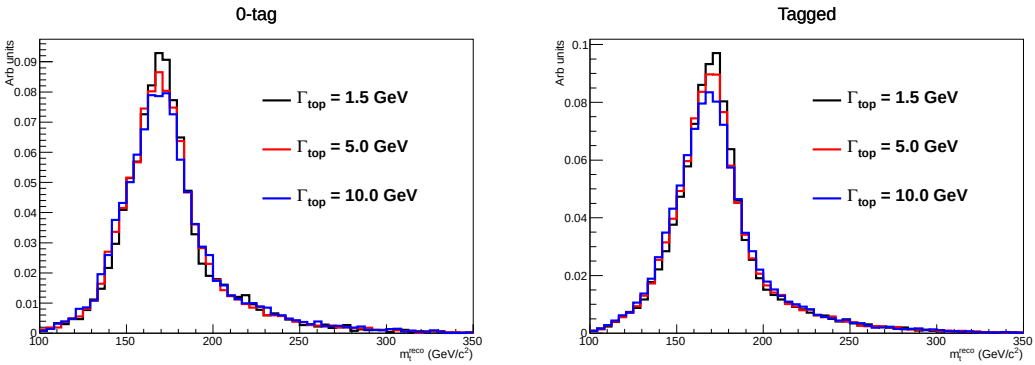

FIG. 1: Reconstructed top quark mass distributions of samples with different input top quark widths: 1.5 GeV, 5.0 GeV and 10.0 GeV.(0-btag events on left plot and tagged events on right plot)

II. DATA SAMPLE AND EVENT SELECTION

This analysis is based on an intergrated luminosity of 8.7 fb^{-1} collected by CDF II detector corresponding to the full data set of CDF Run II.

At trigger level, lepton+jets candidate events are selected by requiring a high-E_T electron (or high-P_T muon). Offline, the events are required to have a single energetic lepton, large missing E_T due to the escaping neutrino from the leptonic W decay, and at least four jets in the final state. Jets are reconstructed with JETCLU[5] cone algorithm using a cone radius of $R \equiv \sqrt{\eta^2 + \phi^2} = 0.4$. To improve the statistical power of the analysis, we divide the lepton+jets samples into five categories depending on the number of jets identified as arising from the hadronization and decay of b quarks as well as the number of tight jets. The SECVTX[6] algorithm uses the transverse decay length of tracks inside jets to tag jets as coming from b quarks. We require at least one tagged jet for lepton+jets events.

We also make a cut on the χ^2 out of the kinematic fitter which will be covered later, requiring it to be less than 9.0 (3.0) for tagged (0-tag) events. In order to properly nomalize our probability density functions we define hard boundaries on the observables, that is, events in which observables with values falling outside of the boundaries are rejected.

III. JET ENERGY SCALE

We describe in this section the *a priori* determination of the jet energy scale uncertainty by CDF that is used later in this analysis. More information about JES, calibration and uncertainty can be found in [7]. There are many sources of uncertainties related to jet energy scale at CDF:

- Relative response of the calorimeters as a function of pseudorapidity
- Single particle response linearity in the calorimeters
- Fragmentation of jets
- Modeling of the underlying event energy
- Amount of energy deposited out of the jet cone

The uncertainty on each source is evaluated separately as a function of the jet p_T (and η for the first uncertainty in the list above). Their contributions are shown in Fig 2 for the region 0.2 ¡ η ¡ 0.6. The black lines show the sum in quadrature (σ_c) of all contributions. This $\pm\sigma_c$ total uncertainty is taken as a unit of jet energy scale miscalibration ($\Delta_{\rm JES}$) in this analysis.

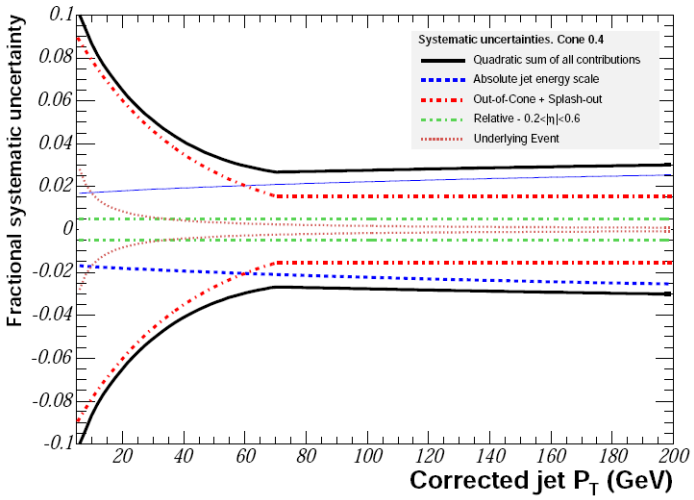

FIG. 2: Jet energy scale uncertainty as a function of the corrected jet p_T for the underlying event(dotted red), relative response (dashed green), out-of-cone energy (dashed red) and absolute response (dashed blue). The contribution of all sources are added in quadrature (full black) to form the total $\Delta_{\rm JES}$ systematic σ_c.

A. Top Quark mass reconstruction

The reconstructed top quark mass ($m_t^{\rm reco}$) in lepton+jets channel is determined by minimizing a χ^2 describing the overconstrained kinematics of the $t\bar{t}$ system. The reconstructed top mass is a number that distills all the kinematic information in each event into one variable that is a good estimator for the true top quark mass. The kinematic fitter uses knowledge of the lepton and jet four-vectors, b-tagging information and the measured missing E_T. The invariant masses of the lepton-neutrino pair and the dijet mass from the hadronic W decay are constrained to be near the well known W mass, and the two top quark masses per event are constrained to be equal within the narrow top width. The χ^2 (Eqn 2) is minimized for every jet-parton assignment consistent with b-tagging. The first sum constrains the p_T of the jets and lepton, within their uncertainties, to remain close to their measured values. The second term constrains the unclustered energy in the event to remain near its measured value, providing a handle on the neutrino 4-vector. The W boson has a small width, and the two W mass terms provide the most powerful constraints in the fit. The last two terms in the χ^2 constrain the three-body invariant masses of each top decay chain to remain close to a single top quark mass, $m_t^{\rm reco}$. The single jet-parton assignment with the lowest χ^2 that is consistent with b-tagging gives the value of $m_t^{\rm reco}$ for the event. Events where the lowest $\chi^2 > 9.0$ (3.0) are rejected for b-tagged events (0-tag events).

$$\begin{aligned}\chi^2 = & \sum_{i=l,4jets} \frac{(p_T^{i,fit} - p_T^{i,meas})^2}{\sigma_i^2} + \sum_{j=x,y} \frac{(p_j^{UE,fit} - p_T^{UE,meas})^2}{\sigma_j^2} \\ & + \frac{(M_{l\nu} - M_W)^2}{\Gamma_W^2} + \frac{(m_{jj} - M_W)^2}{\Gamma_W^2} \\ & + \frac{(M_{bl\nu} - m_t^{\rm reco})^2}{\Gamma_t^2} + \frac{(M_{bjj} - m_t^{\rm reco})^2}{\Gamma_t^2} \end{aligned} \quad (2)$$

IV. DIJET MASS OF W BOSON

The value of m_{jj} in each lepton+jets event can have an ambiguity due to not knowing which two jets came from a hadronic W decay. In 2-tag events, the value is chosen as the invariant mass of the two non-tagged jets in the leading 4 jets. In single-tag events, there are 3 dijet masses that can be formed from the 3 non-tagged jets among the 4 leading jets in the event. In the zero-tag events, there are 12 ijet masses. We choose the single dijet masses that is closest to the well know W mass.

V. BACKGROUNDS

An *a priori* estimate for the Lepton+Jets background composition is used to derive background shapes for $m_t^{\rm reco}$ and m_{jj}. ALPGEN combined with PYTHIA is used to model W+jets. Contributions include Wbb,Wcc, Wc and W+light favor (LF) jets. Non-isolated leptons are used to model the QCD background. The relative fractions of the different W+jets samples are determined in MC, but the absolute normalization is derived from data. The MC are combined using their relative cross sections and acceptances, and we remove events overlapping in phase space and favor across different samples. MC and theoretical cross-sections are used to model the single-top and diboson backgrounds. The expected number of background from different sources is shown in Table I. The backgrounds are assumed to have no $\rm M_{top}$ dependence, but all MC-based backgrounds are allowed to have $\Delta_{\rm JES}$ dependence.

VI. KERNEL DENSITY ESTIMATION

To get the probability density function (p.d.f.) for signals and backgrounds we use Kernel Density Estimation (KDE) instead of simply fitting usual histograms. The (p.d.f.) in this analysis is a two-dimentional function of reconstructed top mass $m_t^{\rm reco}$ and dijet mass of W boson m_{jj}:

$$P(m_t^{\rm reco}, m_{jj} | \Gamma_{\rm top}, \Delta_{\rm JES}) \quad (3)$$

For signal, there is one p.d.f. for each set of $\Gamma_{\rm top}$ and $\Delta_{\rm JES}$, while for background it only has one parameter $\Delta_{\rm JES}$ since backgrounds do not depend on top quark mass. These p.d.f. will finally be needed for the maximum likelihood fit for any PE or data fit.

TABLE I: Expected numbers of background and signal events and observed events after event selection, χ^2 and boundary cuts for each category.

CDF II Preliminary 8.7 fb^{-1}

	0-tag	1-tagL	1-tagT	2-tagL	2-tagT
W+jets	703 ± 199	170 ± 60	102 ± 37	11.6 ± 4.9	8.4 ± 3.5
Z+jets	52.3 ± 4.4	8.9 ± 1.1	5.9 ± 0.7	0.8 ± 0.1	0.5 ± 0.1
Single top	4.8 ± 0.5	10.5 ± 0.9	6.8 ± 0.6	2.2 ± 0.3	1.7 ± 0.2
Diboson	60.3 ± 5.6	111 ± 1.4	8.5 ± 1.1	1.0 ± 0.2	0.8 ± 0.1
Multijets	143 ± 114	34.5 ± 12.6	20.7 ± 16.6	4.4 ± 2.5	2.5 ± 2.4
Background	963 ± 229	235 ± 61	144 ± 41	19.9 ± 5.5	13.8 ± 4.2
$t\bar{t}$ signal	645 ± 86	695 ± 87	867 ± 108	192 ± 30	304 ± 47
Expected	1608 ± 245	930 ± 106	1011 ± 115	212 ± 30	318 ± 47
Observed	1627	882	997	208	275

While histograms are a useful but limited way to estimate p.d.f., KDE supplies a better approach to estimate the underlying density of observed data. A KDE is in fact another histogram-like estimation. It associates to each data point a function (called a kernel function). The kernel histogram (properly normalized) is the sum of all these functions, which typically depend on a parameter called the *bandwidth* that significantly affects the roughness or smoothness of the kernel histogram that is ultimately generated.

VII. LIKELIHOOD FIT

To extract the top quark width from the distribution of reconstructed top mass and dijet mass, we construct a likelihood term:

$$\begin{aligned}\mathcal{L}_{shape} &= \frac{(n_s+n_b)^N e^{-(n_s+n_b)}}{N!} \times e^{-\frac{(n_{b0}-n_b)^2}{2\sigma^2_{n_{b0}}}} \\ &\times \prod_{i=1}^{N} \frac{n_s P_s(m_t^{\rm reco}, m_{jj}; \Gamma_{\rm top}, \Delta_{\rm JES}) + n_b P_b(m_t^{\rm reco}, m_{jj}; \Delta_{\rm JES})}{n_s+n_b}\end{aligned} \tag{4}$$

where n_s and n_b are expected number of signal and background events and N is the total number of events in the sample; P_s and P_b are the probability density function s for signal and background respectively. The first term is present in Equation 4 since this is an extended likelihood, meaning that the number of signal and background events obey Poisson statistics. The second term constrains the number of background events to predicted number n_{b0} within its uncertainty to improve sensitivity. Probability density functions P_s and P_b, which are obtained from Kernel Density Estimation, are used to discern between signal and background event in order to extract top width, based on a minimization of the negative log likelihood.

VIII. A FELDMAN-COUSINS CONSTRUCTION

The key feature in constructing confidence intervals using Feldman-Cousins scheme is to define the *ordering principle*. In [4], an ordering principle is defined per Pesudo-Experiment as likelihood ratio,

$$R(x) = \frac{P(x|\Gamma_0)}{P(x|\Gamma_{max})} \tag{5}$$

, where $R(x)$ is a likelihood ratio at x for a given width, Γ_0, and Γ_{max} is the width that yields the maximum likelihood among all the possible width. For a MC sample we run thousands of Pseudo-Experiments. We then obtain the likelihood ratio and order the PE results based on this values. Therefore we can obtain the confidence band containing 95% or 68% events.

After we built the Feldman-Counsin band from MC samples, we test the coverage by running another set of PEs. The results in Fig. 4 show very nice coverage as we expected in the solid line. Note that we have two parameters when generating MC samples–$\Gamma_{\rm top}$ and $\Delta_{\rm JES}$, thus routinely a two-dimentional Feldman-Cousins construction should be performed. In our analysis, however, we fixed $\Delta_{\rm JES} = 0$ and only $\Gamma_{\rm top}$ is used. We then check the coverage with different $\Delta_{\rm JES}$ in Fig. 5. It shows that we do not have significant difference from difference $\Delta_{\rm JES}$ values.

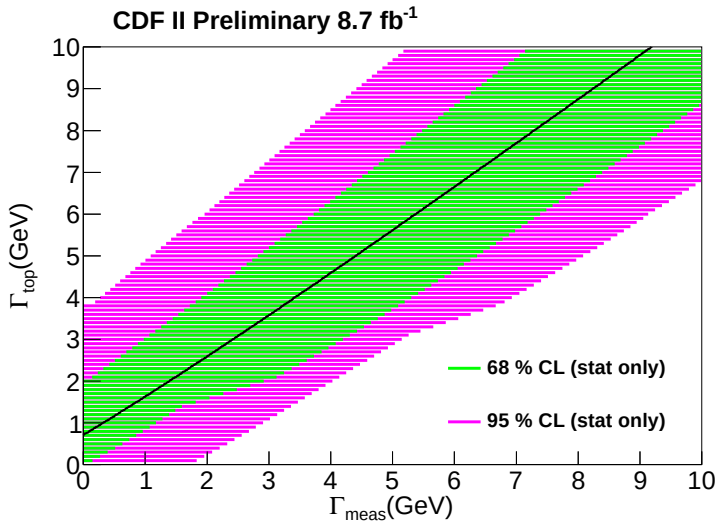

FIG. 3: 68% as well as 95% confidence level Feldman-Counsin band with statistical uncertainties only

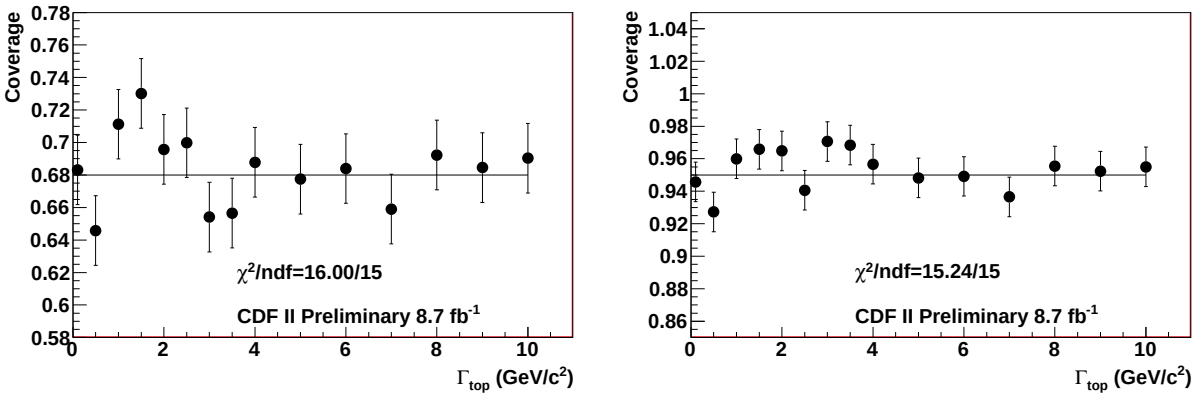

FIG. 4: Coverage test with monte-carlo experiments at 68% (left) and 95% (right) confidence level.

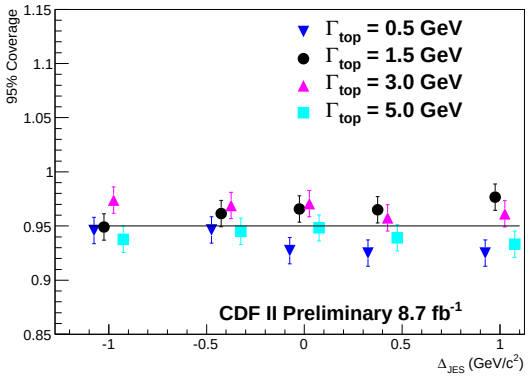

FIG. 5: Coverage test with different $\Delta_{\rm JES}$.

TABLE II: Summary of shift the measured top width due to systematic effects. All numbers have units of GeV.

CDF Run II Preliminary 8.7 fb^{-1}

Systematic	$\Delta\Gamma_{\rm meas}$ (GeV)
Jet Resolution	0.56
Color Reconnection	0.69
Generator	0.50
Higher Order Effect	0.21
Residual Jet Energy Scale	0.19
Parton Distribution Functions	0.24
b Jet Energy Scale	0.28
Background Shape	0.18
gg Fraction	0.26
Radiation	0.17
Lepton Energy	0.03
Multiple Hadron Interaction	0.23
Total Effect	1.22

IX. INCORPORATING SYSTEMATIC EFFECTS

Because we use the reconstructed top mass distributions to extract top width, any systematic that possibly alters the shape and location of the reconstructed top mass distribution will potentially change the fitted top width out of the likelihood fitter. We estimate each uncertainty by performing a series of pseudoexperiments with various systematic MC samples with top mass 172.5 GeV/c^2.

We examine a variety of effects that could systematically shift our measured top width. As a single nuisance parameter, the JES that we measure does not fully capture the complexities of possible jet energy scale uncertainties, particularly those with different η and p_T dependence. Fitting for the global JES removes most of these effects, but not all of them. We apply variations within uncertainties to different JES calibrations for the separate known effects in both signal and background pseudodata and measure resulting shifts in top width $\Gamma_{\rm top}$ from pseudoexperiments, giving a residual JES uncertainty. Jet resolution can change the shape of reconstructed top mass distribution. While we cannot improve the jet resolution in our simulation, we can worsen it by smearing the jet resolution with a Gaussian function. We smear the jet resolution with a Gaussian probability density function with σ that is 5% of our default jet resolution. We also vary the energy of b jets, which have different fragmentation than light quarks jets, as well as semi-leptonic decays and different color flow, resulting in a b-JES systematic. Effects due to uncertain modeling of radiation including initial-state radiation (ISR) and nal-state radiation (FSR) are studied by extrapolating uncertainties in the p_T of Drell-Yan events to the $t\bar{t}$ mass region, resulting in a radiation systematics. Comparing pseudoexperiments generated with HERWIG and PYTHIA gives an estimate of the generator systematic. A systematic on different parton distribution functions is obtained by varying the independent eigenvector of the CTEQ6M set, comparing parton distribution functions with different values of QCD, and comparing CTEQ5L with MRST72. We also test the effect of reweighting MC to increase the fraction of tt events initiated by gg (vs qq) from the 6% in the leading order MC to 20%. Systematics due to lepton energy scales are estimated by propagating 1% shifts on electron and muon energies scales. Background composition systematics are obtained by varying the fraction of the different types of backgrounds in pseudoexperiments. For Lepton+Jets backgrounds, varying the uncertain Q^2 of background events results in a background shape systematic, and using a different model for QCD events gives an additional QCD modeling systematic. It has been suggested that Color Reconnection (CR) effects could cause a bias in the top quark mass measurement. We test this effect by generating MCs with and without CR and take the difference as systematics. The dependence of measured top width on input top mass could also contribute to systematic effects, but after performing some PEs with different input top masses we find that the measurement of top width is insensitive to top mass therefore we simply ignore its effect in this analysis.

The shift of the measured top width due to total systematic effects is 1.22 GeV. The summary of systematics is in Table II .

In order to incorporate these systematic effects into top width limit(s), we first use a convolution method for folding systematic uncertainties into likelihood function. That is, we convolute the original probability density function PDF_0(pure statistic) with a Gaussian function related to systematic effects to obtain a new probability density function PDF:

$$PDF(\Gamma_{top}|x) = \int d\tilde{\Gamma}_{top} PDF_0(\tilde{\Gamma}_{top}|x) \frac{e^{-\frac{1}{2}(\frac{\tilde{\Gamma}_{top}-\Gamma_{top}}{\sigma})^2}}{\sqrt{2\pi}\sigma} \tag{6}$$

where x represents data and σ is equal to the total top width shift(1.22 GeV) due to systematic effects.

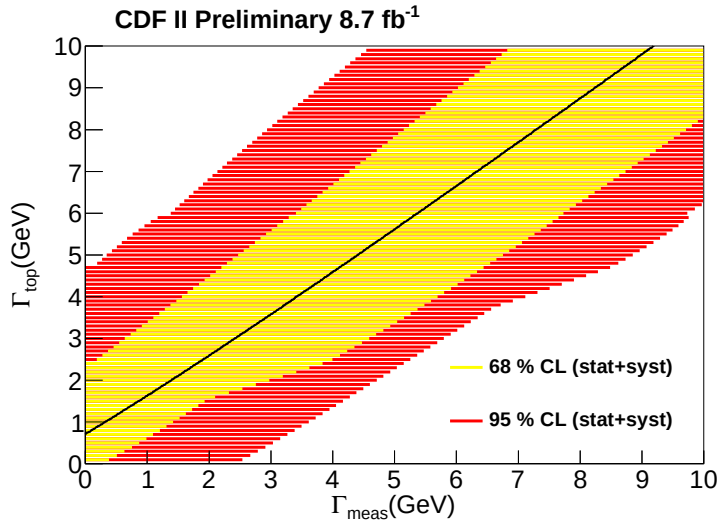

FIG. 6: 68% as well as 95% confidence level Feldman-Counsin band with stat+syst uncertainties

X. RESULTS

We use dataset collected at CDF until the shutdown, corresponding to a total integrated luminosity of $8.7 fb^{-1}$. We obtain the measured top quark width from data to be 1.63 GeV as shown in Fig. 7.

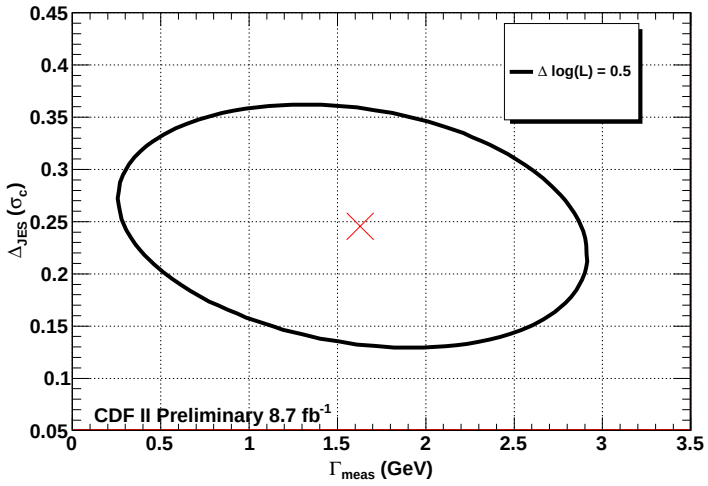

FIG. 7: 2D Log-likelihood fit of data with one standard deviation contour and best fit point is shown.

Figure 8 shows the distributions of the reconstructed top mass and dijet mass for the dataset, overlaid with probability density functions from input $\Gamma_{\rm top} = 1.5$ GeV and full lepton+jets backgrounds.

After performing the log-likelihood fit of data, the $\Gamma_{\rm top}$ result of data (1.63 GeV) can be interpreted as $\Gamma_{\rm top}$ using already built Feldman-Counsin bands. Figure 9 show the Feldman-Counsin band with the best fit point as arrow. We find an upper limit of the top quark width $\Gamma_{\rm top} < 6.38$ GeV at 95% confidence level. We also have two side limit of

$1.11 < \Gamma_{\rm top} < 4.05$ GeV at 68% confidence level. With the Feldman-Counsin band as well as the most probable value in the solid line of the figure, we can obtain,

$$\Gamma_{\rm top} = 2.21^{+1.46}_{-0.92}({\rm stat})^{+1.12}_{-0.62}({\rm syst}){\rm GeV} = 2.21^{+1.84}_{-1.11}{\rm GeV}.$$

We can convert the top quark width to the top quark lifetime using the relation of $\Gamma_{\rm top} \times \tau_{\rm top} = \hbar$. We can set the 95% CL low limit as $\tau_{\rm top} > 1.03\times10^{-25}$ s as well as two side bound with 68 % CL as $1.63\times10^{-25} < \tau_{\rm top} < 5.98\times10^{-25}$ s. We also obtain,

$$\tau_{\rm top} = 2.98^{+3.00}_{-1.35} \times 10^{-25}{\rm s}$$

.

XI. CONCLUSIONS

We present a measurements of top quark width using the full data set of CDF Run II corresponding to an integrated luminosity of 8.7 fb^{-1} $p\bar{p}$ collisions at Tevatron. We measure a top quark width to be $\Gamma_{\rm top} = 2.21^{+1.84}_{-1.11}$ GeV. We also set the 95 % CL upper limit of 6.38 GeV. The $\Gamma_{\rm top}$ result can be converted into the top quark life time of $\tau_{\rm top} = 2.98^{+3.00}_{-1.35} \times 10^{-25}$s.

Acknowledgments

We thank the Fermilab staff and the technical staffs of the participating institutions for their vital contributions. This work was supported by the U.S. Department of Energy and National Science Foundation; the Italian Istituto Nazionale di Fisica Nucleare; the Ministry of Education, Culture, Sports, Science and Technology of Japan; the Natural Sciences and Engineering Research Council of Canada; the National Science Council of the Republic of

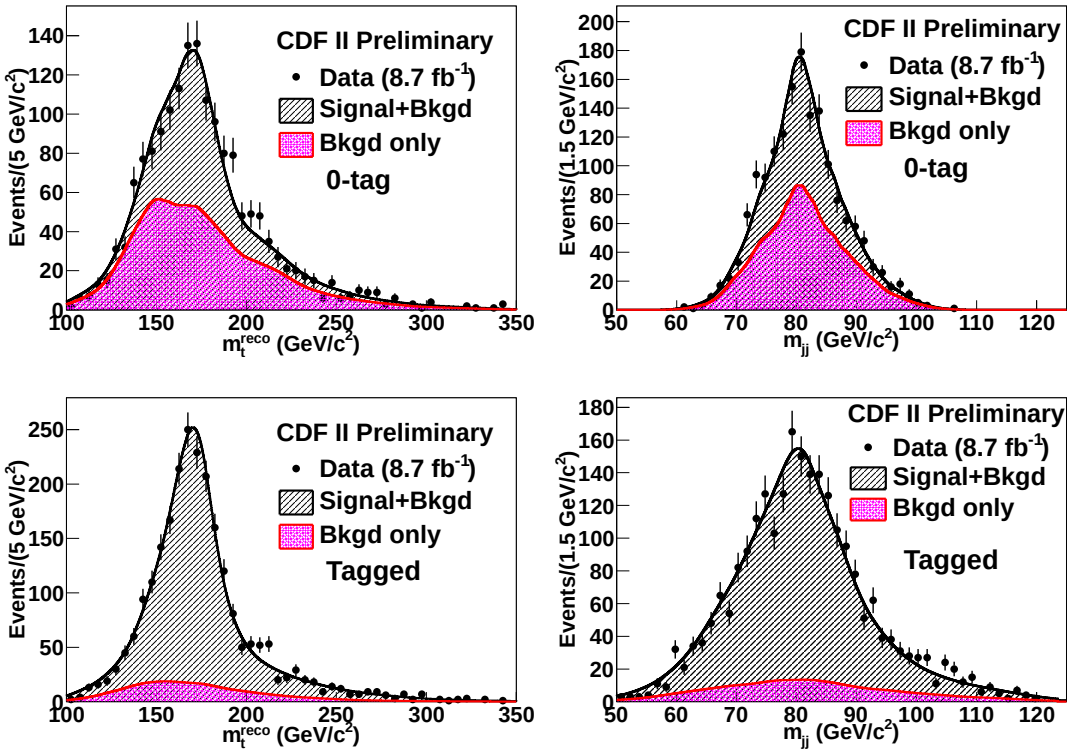

FIG. 8: One-dimensional 0-tag (up) and tagged (down) data templates with PDFs from $\Gamma_{\rm top} = 1.5$ GeV/c^2 and full background models overlaid. The extracted numbers of events are set to the value from data fit.

China; the Swiss National Science Foundation; the A.P. Sloan Foundation; the Bundesministerium fur Bildung und Forschung, Germany; the Korean Science and Engineering Foundation and the Korean Research Foundation; the Science and Technology Facilities Council and the Royal Society, UK; the Institut National de Physique Nucleaire et Physique des Particules/CNRS; the Russian Foundation for Basic Research; the Ministerio de Ciencia e Innovacion, and Programa Consolider-Ingenio 2010, Spain; the Slovak R&D Agency; and the Academy of Finland.

[1] M.Jezabek and J.H.Kuhn, Nucl.Phys.B 314,1 (1989)
[2] I.I.Y. Bigi et al., Phys.Lett.B181, 157 (1986)
[3] Aaltonen et al. (The CDF Collaboration), Phys. Rev. Lett., 105, 232003 (2010)
[4] G.Feldman and R.Cousins, Phys.Rev.D 57, 3873 (1998)
[5] F.Abe, et al., Phys.Rev.D 45, 1448 (1992)
[6] T.Affolder, et al., Phys.Rev.D 64, 032002 (2001)
[7] A.Bhatti,et al.,Nucl.Instrum.Methods Phys.Rev.A 566,375 (2006)

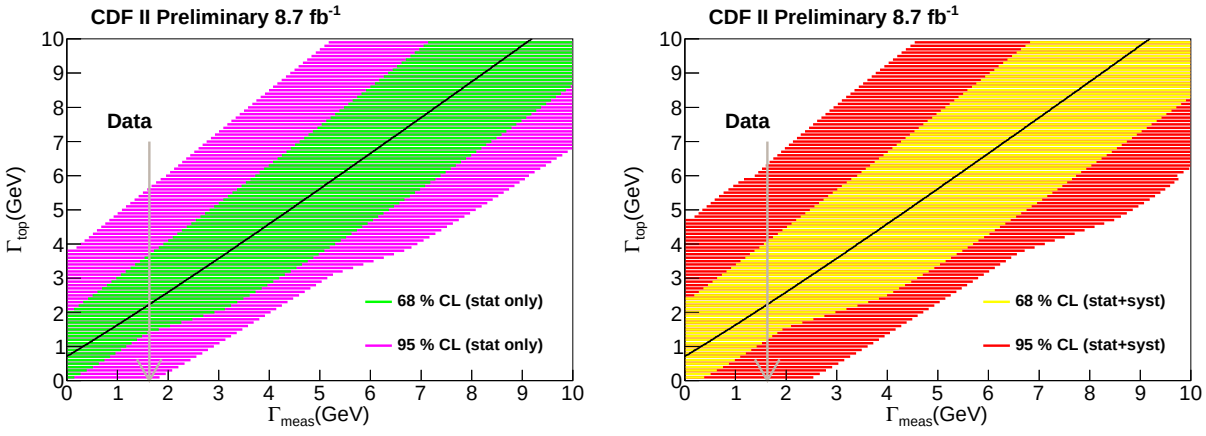

FIG. 9: Confidence band of statistical uncertainty only (left) and stat+syst uncertainty (right) are shown with data (arrow).